

# Supramolecular organization of photosynthetic membrane proteins in the chlorosome-containing bacterium *Chloroflexus aurantiacus*

David Bína · Zdenko Gardian · František Vácha · Radek Litvín

Received: 31 January 2014 / Accepted: 8 April 2014 / Published online: 24 April 2014  
© Springer Science+Business Media Dordrecht 2014

**Abstract** The arrangement of core antenna complexes (B808-866-RC) in the cytoplasmic membrane of filamentous phototrophic bacterium *Chloroflexus aurantiacus* was studied by electron microscopy in cultures from different light conditions. A typical nearest-neighbor center-to-center distance of ~18 nm was found, implying less protein crowding compared to membranes of purple bacteria. A mean RC:chlorosome ratio of 11 was estimated for the occupancy of the membrane directly underneath each chlorosome, based on analysis of chlorosome dimensions and core complex distribution. Also presented are results of single-particle analysis of core complexes embedded in the native membrane.

**Keywords** Photosynthesis · LH1 · Chlorosome · Macromolecular crowding · Electron microscopy · *Chloroflexus aurantiacus*

## Abbreviations

B808-B866	The core antenna of <i>Chloroflexus aurantiacus</i>
<i>Cfx</i>	<i>Chloroflexus</i>
FAP	Filamentous anoxygenic phototrophs
LH1, LH2	Light-harvesting complexes of purple bacteria
<i>P</i>	Primary donor of the reaction center

$Q_A$	1st quinone acceptor of the reaction center
RC	Reaction center

## Introduction

The photosynthetic apparatus of filamentous anoxygenic phototrophs (FAP) such as *Chloroflexus (Cfx.) aurantiacus* appears to be a peculiar combination of components from purple bacteria and green sulfur bacteria. At the heart of the photosystem is a (mena-)quinone-reducing purple-like reaction center (RC), composed of two subunits corresponding to L and M proteins of purple bacterial RC, binding 3 bacteriochlorophyll *a* (BChl *a*) and 3 molecules of bacteriopheophytin (Ovchinnikov et al. 1988a, b; Blankenship et al. 1983). The notable absence of the third subunit, H, makes it the simplest known photosystem II-type reaction RC.

The RC is surrounded by a circular multimeric antenna composed of dimers of helices in a manner of LH1 but binding three, instead of two, molecules of BChl *a* per dimeric subunit, arranged in two spectrally distinct groups, monomeric B808, and excitonically coupled B866, similar to LH2. Uncertainty concerning the number of antenna subunits remains. In the work of Xin et al. (2005), the core complex was envisioned as consisting of a dimer of RCs, surrounded by a 12 subunit antenna based on biochemical methods and analysis of electron microscopy images showing a particle of ~22 nm diameter. However, later works did not support this interpretation. Utilizing small-angle X-ray scattering Tang et al. (2010) found a particle with diameter of ~13 nm, close to the purple bacterial LH1-RC complex (Roszak et al. 2003). Moreover, analysis

D. Bína (✉) · Z. Gardian · F. Vácha · R. Litvín  
Faculty of Science, University of South Bohemia, Branišovská  
31, 37005 České Budějovice, Czech Republic  
e-mail: bina@umbr.cas.cz

D. Bína · Z. Gardian · F. Vácha · R. Litvín  
Biology Centre ASCR vvi, Institute of Plant Molecular Biology,  
Branišovská 31, 37005 České Budějovice, Czech Republic

of the core complex of a related species, *Roseiflexus castenholzii*, also yielded parameters close to the complex from purple bacteria, ~13 nm diameter,  $15 \pm 1$  subunits (Collins et al. 2010).

In the majority of known FAP species, the core complex is accompanied by external antenna complex typical of green bacteria, the BChl *c*-containing chlorosome, although without any additional complexes similar to the FMO protein of green sulfur lineage.

The exact geometry of the organization of the core complexes in the cytoplasmic membrane of FAP is not known; the only available information reports approximate RC:chlorosome stoichiometries based on pigment ratios (Golecki and Oelze 1987). Also unknown is the exact mechanism of chlorosome development (Hohmann-Marriott and Blankenship 2007; Pedersen et al. 2010) as is its relation to RC and core antenna complex assembly.

The primary aim of the present work was to address the first of the above-stated closely related questions. Direct observations of supramolecular organization of the membrane complexes in filamentous anoxygenic phototroph are presented and analyzed, and the likely core:chlorosome stoichiometry is derived. The effect of varying growth light intensity upon spatial distribution of core complexes was also studied. Moreover, in order to settle the question of core complex dimensions, single-particle analysis of the core complex of *Cfx. aurantiacus* embedded in native membrane was performed. Combined with optical spectroscopy, the analysis indicated that the native core complex of *Cfx. aurantiacus* is likely about 10 nm in diameter with 16 antenna subunits per RC (c.f. Tang et al. 2010; Collins et al. 2010). The implications of the observed arrangement of the core complexes in the cytoplasmic membrane are discussed against the background of purple bacterial system, e.g., LH1-RC from *Rhodospseudomonas viridis* (e.g., Miller 1979).

## Materials and methods

### Cultivation

Cells of *Cfx. aurantiacus* J-10-fl were grown anaerobically for 4–5 days in 25-mL screw-capped flasks under 60 W incandescent light bulb at moderate ( $22 \mu\text{mol photons m}^{-2} \text{s}^{-1}$ ) or high ( $50 \mu\text{mol photons m}^{-2} \text{s}^{-1}$ ) irradiance inside a temperature controlled shaker (Innova 44, Eppendorf, Germany) at 50 °C.

### Membrane isolation

Membranes were prepared by breaking cells using EmulsiFlex-C5 (Avestin Inc., Canada) at 20,000 psi. After

removal of unbroken cells by low speed centrifugation, membranes were pelleted at  $60,000 \times g$  and resuspended in 50 mM Tris-HCl, pH 8.

### Electron microscopy

Freshly prepared membranes were used immediately for transmission electron microscopy (TEM). Specimens were placed on glow-discharged carbon-coated copper grids and negatively stained with 2 % uranyl acetate. TEM was performed using a JEOL JEM-2100F transmission electron microscope (JEOL, Japan) at 200 kV equipped with bottom-mount Gatan Orius SC1000 CCD camera (Gatan Inc., USA). Single-particle analysis was performed on 823 manually selected particles using the Spider and Web software package (Frank et al. 1996). No bandpass filtering was applied to particle images prior to averaging. Other numerical analyses were done using locally written MATLAB<sup>®</sup> (Mathworks Inc., USA) scripts. Comparison of distributions was done using quantile–quantile (q–q) plots. Statistical testing was done using *t* test (for normal data), or by bootstrap approach (Efron 1979), whereby the probability density function of the test statistics (e.g., a difference between medians of the two datasets) was constructed from pairs of populations obtained by resampling with replacement of the experimental datasets. The null hypothesis (identity of the populations) was rejected if the value of the test statistics computed from the input data fell outside of the 5 % confidence interval of the bootstrap distribution.

### Spectroscopy

Steady-state absorption spectra were measured using UV-2600 spectrometer equipped with an integration sphere ISR-2600Plus (Shimadzu, Japan). Time-resolved light-induced absorbance changes were measured on the same sample that was used for electron microscopic analysis using a locally built kinetic spectrometer described earlier (Bina et al. 2006, 2010) using TTL-triggered 850 nm LED as actinic light source (M850L2, Thorlabs Inc., USA).

## Results and discussion

Cells of *Cfx. aurantiacus* form long filaments, approximately 350 nm in diameter with individual cells several micrometers long. Upon disruption, the cytoplasmic membrane of the cells broke into flat pieces up to hundreds of nanometers across. These sheets of membrane were collected by medium speed centrifugation, immediately stained and observed by electron microscopy. About

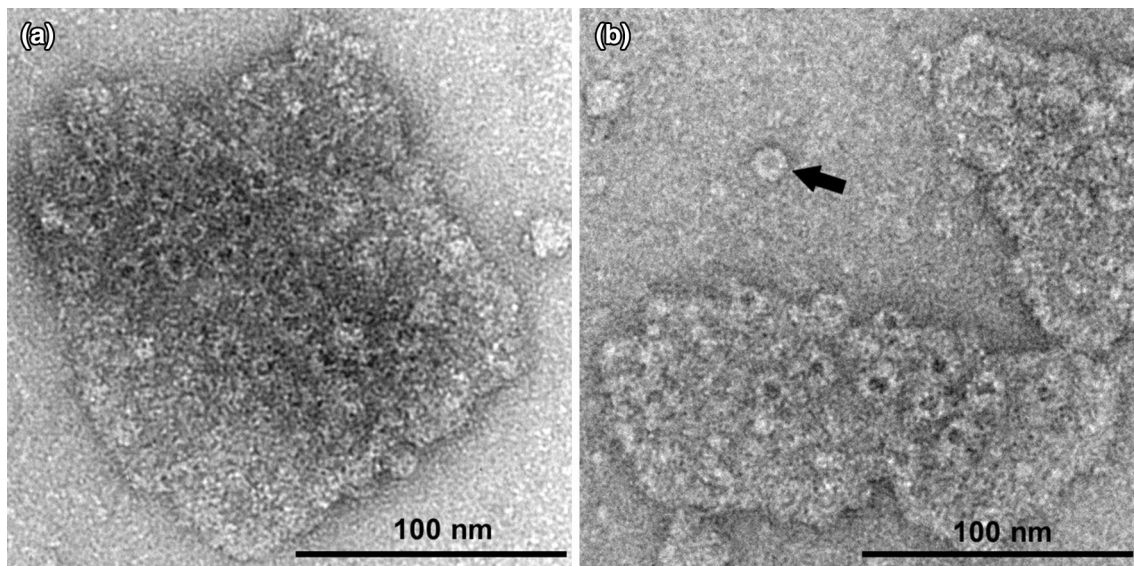


**Fig. 1** Examples of membrane fragments obtained from *Cfx. aurantiacus*, containing the B808-866-RC (core) complexes, visible as rings. **a** Array of cores completely enclosed in the membrane;

**b** Membrane sheet broken off in a way that partially exposed the core complexes. A fully detached core is visible in the *upper left* part of the figure, indicated by *arrow*. Scale bar corresponds to 100 nm

75–80 % of the observed membrane fragments were smaller than 40,000 nm<sup>2</sup>.

Occasionally, membrane patches with chlorosomes still attached were observed, often with several chlorosomes in close contact (not shown). The dimensions of chlorosomes in moderate-light (22 microeinsteins) culture were ( $\pm$ standard deviation) 118( $\pm$ 19)  $\times$  34( $\pm$ 5) nm ( $n = 32$ ) in agreement with published data (e.g., Adams et al. 2013; Psencik et al. 2009). The observation of chlorosomes indicated that the membrane patches were oriented with their cytoplasmic side facing up.

Many membrane sheets clearly showed groups of circular structures, approximately 10 nm in diameter that were interpreted as the B808-866 core antenna complexes, Fig. 1.

#### Analysis of spatial distribution of core complexes

From images such as those presented in Fig. 1, spatial information of 512 particles in 43 membrane patches was collected and analyzed. The absorption spectrum of the culture is given in Fig. 2a. Figure 2b presents the distribution of distances to nearest neighbor of the core complexes. The median of the distribution was  $\sim$ 18 nm, a rather unexpected value corresponding to about 2 $\times$  the core diameter.

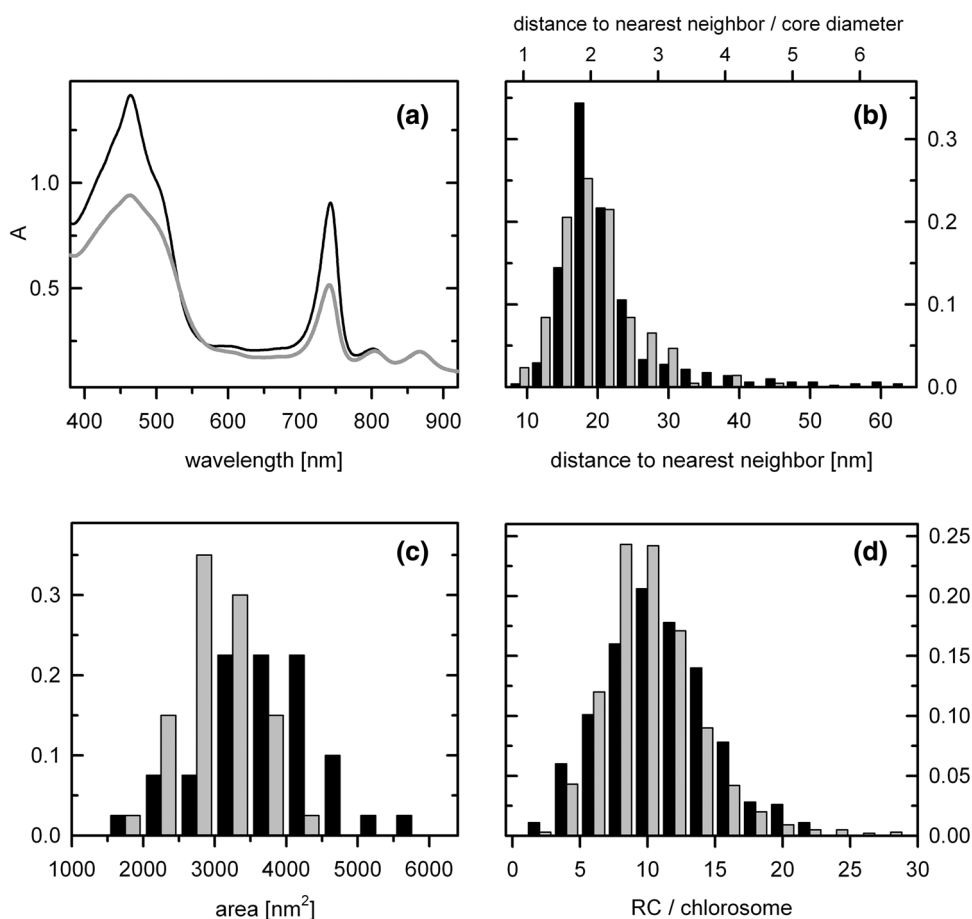
The results described above held also for samples treated with KSCN to enhance the release of chlorosomes from the membrane, as well as samples frozen and thawed prior to isolation, indicating robustness of the observed arrangement of B808-866-RC complexes.

It has been repeatedly demonstrated that in both bacterial and thylakoid photosynthetic membranes there exists significant protein crowding (e.g., Scheuring et al. 2005; Kirchhoff 2008). An early example was presented in the electron microscopic studies of the *Blastochloris* (formerly *Rhodospseudomonas*) *viridis* membranes (Miller 1979) that showed tight packing of the core complexes into hexagonal arrays; this observation was later confirmed by AFM (Scheuring et al. 2003). For such a sample, the plot in Fig. 2b would consist of a very narrow peak centered close to value equal to core antenna diameter.

One can expect that the relatively sparse arrangement of core complexes in *Cfx. aurantiacus* has important consequences for energy and electron transfer. The typical closest center-to-center distance of  $\sim$ 18 nm leads to separation of  $\sim$ 8 nm between BChl *a* pigments of B866 rings. Considering the time constant of LH2-LH2 energy transfer 3–5 ps found in purple bacteria (Agarwal et al. 2002; Olsen et al. 2008), the greater BChl–BChl distance observed in *Cfx. aurantiacus* would cause the inter-antenna energy transfer to slow down by at least two orders of magnitude. Consequently, considering the trapping time in the tens of picosecond range, the energy migration in such system likely consists mainly of vertical, baseplate to core transfer (rate constant of this process is up to  $\sim$ 40 ps, Causgrove et al. 1990; Muller et al. 1993; Fetisova et al. 1996), with lateral excitation diffusion limited mostly to single nearest neighboring B808-866 unit.

It has been shown that the proteins determine the geometry of the lipid bilayer in which they are embedded (e.g., Hsin et al. 2010). It is thus possible that increased spacing of

**Fig. 2** Comparison of organization of membrane of moderate (black) and high-light (gray) cultures of *Cfx. aurantiacus*. **a** Absorption spectra of whole cells; **b** Histogram showing the distribution of the distance to nearest neighbor for the core complexes. Note the typical distance of  $\sim 1.8 \times$  core diameter; **c** Distribution of chlorosome areas; **d** Distribution of RC:chlorosome ratio computed using distribution of nearest-neighbor distances and chlorosome dimensions, for explanation see text



cores is necessary to maintain flat membrane structure required to ensure proper contact of B808-866-RC with the baseplate, likely a rigid planar structure (Psencik et al. 2009). Another reason for the observed core complex distribution may lie in the properties of the electron transfer machinery. Although some uncertainty concerning this issue remains (Majumder et al. 2013), auracyanins are the most likely mobile electron donors to the RC. It was shown that auracyanins in *Cfx.* are membrane anchored. Hence, it is possible that the lipid environment separating the core complexes is necessary to allow diffusion of the membrane-anchored mobile electron carriers to all reaction centers. Moreover, the same mechanism might also serve the purpose of limiting the mobility of the electron carriers to certain membrane domains, since the photosynthetic membrane of *Cfx. aurantiacus* lines the inner surface of the cell, not forming the (semi)enclosed vesicular structures observed in purple bacteria. Unfortunately, we failed to identify the alternative complex III, paralleling the long-standing problem of localization of the cytochrome  $bc_1$  complex in the membrane of purple bacteria, an issue resolved only very recently (Carson et al. 2014).

In order to see whether the spatial organization of core complexes related to amount of BChl *c*, the cells were

cultivated under irradiance increased 2 times. As seen in Fig. 2a, the culture maintained under elevated irradiance showed an approximate 2-fold decrease in absorbance of the chlorosome relative to the core. Using the amplitude of light scattering measured outside of range of BChl absorption (950 nm) as a rough indicator of cell concentration, it was estimated that the amount of B808-866-RC per cell increased by about 20 % compared to cells from moderate light. The distribution of distance to nearest-neighbor parameter corresponding to this “high-light” culture is plotted in gray bars in the Fig. 2b. Compared to the moderate-light culture, the distribution was markedly flatter (a statistically significant difference of kurtosis was found) but the median was not significantly changed. The chlorosomes of high-light cells were found to be slightly shorter  $94(\pm 14) \times 33(\pm 5)$  nm ( $n = 40$ ), in agreement with earlier reports (Golecki and Oelze 1987). Histograms comparing the areas of the top-view projections of chlorosomes of both cultures are given in Fig. 2c.

Chlorosome dimensions and spatial statistics of the core complexes were further used to estimate the likely RC:chlorosome ratios for each of our *Cfx.* cultures. First, a set of 1,000 shapes constructed as rectangles with semi-circles at a pair of opposite sides (*cf.* Golecki and Oelze



1987) to represent chlorosomes was generated based on random sampling of datasets of observed chlorosome widths and lengths. For each “chlorosome,” the simulation started by a random placement of a core within the shape. Other cores were then added sequentially using distances sampled randomly from the observed distribution of nearest-neighbor distances (Fig. 2b). The outer limit for RC placement was set to the outline of the chlorosome. Each deposited core was assigned a circular area with a diameter equal to its nearest-neighbor distance to eliminate this area for placement of another core. The simulation for each “chlorosome” terminated when the union of the nearest-neighbor distance circles covered the whole “chlorosome.” Correspondence of the simulated nearest-neighbor data to the experimental statistics was afterwards verified using q–q plot. The results of this simulation, given in Fig. 2d, suggested that the differences in chlorosome areas were compensated for by changes in core complex distributions to maintain the mean RC : chlorosome ratio of  $\sim 11$ . When the available area for core placement was enlarged to account also for the possibility for the cores to be in contact chlorosome outline from the outside, the mean RC:chlorosome ratio increased to  $\sim 14$ .

The data in Fig. 2d are based only upon directly observable quantities (nearest-neighbor distance, chlorosome dimensions) using minimal assumption of full chlorosome area occupancy and thus provide a reliable conservative limit on the density of core complexes under the chlorosome baseplate. However, it does not satisfactorily address the possibility of presence of cores localized in the cytoplasmic membrane separately from chlorosomes. Analysis of pigment content provides a suitable tool in this respect. Such investigation was already performed by Golecki and Oelze (1987) who combined pigment analyses with precise morphometric measurements to obtain estimates of concentration of both BChl *a* and BChl *c* per chlorosome in a range of cultures. In order that our results can be compared to the earlier work, we quantified BChl *a*:BChl *c* ratios for our high-light and moderate-light cultures. These, along with the respective baseplate areas, and the RC : chlorosome ratios are given in Table 1. For reader’s convenience, we also summarized the results of Golecki and Oelze (taken from the Table 1 of the cited article). As seen in Table 1, the inferred numbers of RC per chlorosomes in the 1987 work ranged between 45 and 78. In order that both our method and the pigment-based approach are correct, it must be assumed that the majority of RCs are localized free in the cytoplasmic membrane rather than under the chlorosome baseplate. This is contrary to expectation and also not supported by our observation of a rather large spacing between the core complexes. Thus, a more detailed discussion of this issue is warranted. In the following section, we demonstrate that

the discrepancy can be eliminated if current knowledge of the structure of the components of the photosynthetic apparatus of FAP is used in the analysis of the original data of Golecki and Oelze.

In order that the number of RCs (or cores) relative to the chlorosome can be estimated from the pigment concentration, two parameters must be known: (i) number of BChl *a* molecules per RC (core); (ii) amount of BChl *a* in the baseplate. Two different approaches to problem (ii) are presented in the following section.

In the cited work, 20 BChl *a* per RC were counted, and the ratio BChl *c*:BChl *a*(baseplate) was assumed to be fixed and equal to 25. Then, the number of RC’s per chlorosome was computed as  $([\text{BChl } a] - [\text{BChl } c]/25) \times 1/20$ . The 25:1 ratio was taken from the work of Feick et al. (1982) who obtained it from analyses of isolated chlorosomes. However, it was shown later (Wittmershaus et al. 1988) that no less than 50 % of BChl *a* could be lost from the baseplate when the chlorosome isolation was not done under anaerobic conditions. Consequently, BChl *c*:BChl *a*(baseplate) stoichiometry should be decreased appropriately. Moreover, considering the current opinions about the organization of the core complex in FAP (Xin et al. 2005; Collins et al. 2010; Tang et al. 2010), there should be in total  $3N + 3$  BChl *a* molecules per single core complex that contains a *N*-meric circular antenna; e.g., for a 16-meric complex, there are 16 B808 BChl *a*,  $16 \times 2$  B866 BChl *a*, and 3 BChl *a* in the RC (Blankenship et al. 1983; Pierson and Thornber 1983); that is, 51 BChl *a* molecules per RC whereas the value of 20 corresponds more closely to the RC of green sulfur bacteria.

Applying these modified values to Golecki and Oelze’s BChl concentrations, one arrives at RC to chlorosome ratios that are as much as 4 times smaller than those in the original publication and thus in much better agreement with our data.

Moreover, the very idea of constant ratio of BChl *a* in the baseplate to chlorosome BChl *c* is not self-evident. BChl *a* in chlorosome is located in the baseplate, a planar aggregate of a 5.7 kDa protein (CsmA). A detailed structure of the baseplate has not yet been experimentally determined; however, recent molecular dynamics simulation (Huh et al. 2014) suggested the area density of a dimer consisting of 2 CsmA proteins per  $\sim 11 \text{ nm}^2$ , using the structure of the protein of the green sulfur bacterium *Chlorobaculum tepidum*. A structural element, likely a dimer, of comparable dimensions (3.3 nm) was found earlier in the baseplate of *Cfx. aurantiacus* (Psencik et al. 2009). Moreover, it was shown that the stoichiometry in *Cfx. aurantiacus* baseplate is about 1 CsmA to  $\sim 1.6$  BChl *a*, consistent with  $\sim 3.2$  BChl *a* per dimer (Montano et al. 2003). Hence, the baseplate area can be used to estimate the concentration of bound BChl *a*, and consequently the corresponding RC:chlorosome ratio. Using the

**Table 1** Comparison of baseplate areas, pigment contents, and RC: chlorosome stoichiometries of different *Cfx. aurantiacus* cultures

Sample	Baseplate area [nm <sup>2</sup> ]	[BChl <i>a</i> ] per chlorosome	[BChl <i>c</i> ] per chlorosome	[BChl <i>a</i> ] ÷ [BChl <i>c</i> ]	RC per chlorosome				
1 HL	2,970 ± 560	n.d.	n.d.	0.64 <sup>a</sup>	11 ± 3 <sup>b</sup>				This work
ML	3,750 ± 790			0.35 <sup>a</sup>	11 ± 4 <sup>b</sup>				
2	3,220 ± 840 (2,770–3,810)	1,480 ± 165 (1,222–1,699)	8,184 ± 4,835 (1,392–15,772)	0.34 ± 0.3 (0.11–1.09)	58 ± 12 <sup>c</sup> (45–78)	16 ± 8 <sup>d</sup> (7–28)	11 ± 4 <sup>e</sup> (5–18)	Golecki and Oelze (1987)	

(1) Cultures used in this study, HL, ML: cells grown under 50 μmol photons m<sup>-2</sup> s<sup>-1</sup> and 22 μmol photons m<sup>-2</sup> s<sup>-1</sup>, respectively. See Fig. 2 for graphical presentation of the data; (2) summary of parameters for 8 different cultures from the work of Golecki and Oelze (1987). For more precise appreciation of the distribution of the cited data, both mean ± standard deviation and the ranges (in brackets) are given

<sup>a</sup> Ratios determined from bulk concentrations

<sup>b</sup> Determined from the analysis of TEM images, for explanation see text

<sup>c,d,e</sup> Estimated from pigment concentrations taken from Golecki and Oelze (1987); RC per chlorosome = ([BChl *a*] -  $N_{\text{baseplate}}$ )/ $N_{\text{RC}}$ , where  $N_{\text{baseplate}}$  number of BChl *a* molecules per chlorosome baseplate,  $N_{\text{RC}}$  number of BChl *a* molecules per core complex

<sup>c</sup>  $N_{\text{baseplate}} = [\text{BChl } c]/25$ ,  $N_{\text{RC}} = 20$ ; original parameters used by Golecki and Oelze (1987)

<sup>d</sup>  $N_{\text{baseplate}} = [\text{BChl } c]/12$ , based on Feick et al. (1982) and Wittmershaus et al. (1988);  $N_{\text{RC}} = 51$ , assuming 16-meric B808-866 (16 × 3 BChl *a*) complex surrounding the RC (3 BChl *a*)

<sup>e</sup> assuming  $N_{\text{baseplate}}$  proportional to baseplate area,  $N_{\text{baseplate}} = \text{area [nm}^2\text{]}/(11 \text{ [nm}^2\text{]}) \times 3.2$ , for explanation of parameters of computation see text;  $N_{\text{RC}} = 51$

above given values of 3.2 BChl *a*/(11 nm<sup>2</sup>) for the baseplate leads to RC:chlorosome ratio in good agreement with our estimates of the number of core complexes located within the baseplate area (~11, Table 1). Moreover, the spread of the inferred RC:chlorosome stoichiometries is lower than in the method assuming a fixed ratio between BChl *c* and BChl *a*, which is also in agreement with our observations.

Importantly, neither of above given analyses of pigment contents supports the presence of a large pool of core complexes in areas of the cytoplasmic membrane devoid of chlorosomes, although the presence of some unattached core complexes cannot be excluded, especially considering the observation of complexes spaced as far as 60–70 nm apart (Fig. 2b). On the other hand, the slightly more closely spaced cores in the high-light culture (Fig. 2b, gray bars) might allow for the core arrays to spread to some extent beyond the chlorosome outline while maintaining the efficient lateral excitation transfer.

This problem leads to a question whether the chlorosome baseplate assembles around (or more correctly above) the patch of B808-866-RC complexes or the cores are placed under a pre-formed chlorosome base. In the former case, the free cores, if present, might correspond to future chlorosome-assembly spots. This is a matter of further research.

#### Properties of individual complexes

Hand-picked individual images of core complexes were further subjected to single-particle analysis in order to estimate their dimensions more precisely. In some cases, as

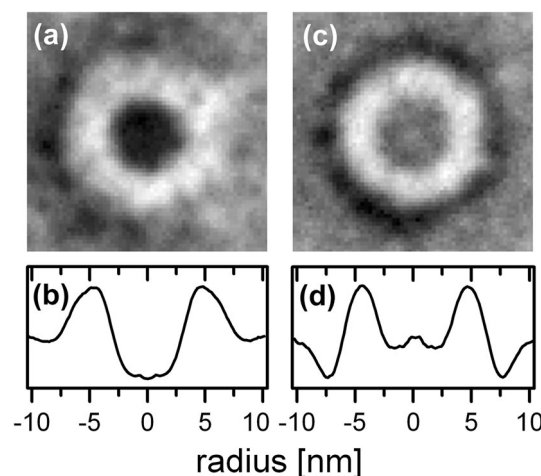


**Fig. 3** Averaged top-view projection maps of B808-866-RC complexes. **a** Representative average of the core complex from *Cfx. aurantiacus* embedded in the native membrane ( $n = 63$ ); **b** Radially symmetrized cross-sectional profile of the particle in **a**. **c** Representative average of the free core complex released from the membrane ( $n = 52$ ); **d** Profile of the particle in **c**

seen in Fig. 1b, the pieces of plasma membrane broke in such a way as to expose the core complexes that were occasionally released from the membrane and found individually on the carbon grids. Both the embedded and the “orphaned” cores were analyzed, Fig. 3. The core complexes were approximately circular, and the apparent diameter of the complex was ~9.4 nm, measured as maximum-to-maximum distance in the cross-section plots in Fig. 3b,d. The dimensions of the core complex are in

agreement with the more recent estimations of the *Cfx.* core diameter (Tang et al. 2010) rather than the value of  $\sim 22$  nm reported earlier (Xin et al. 2005).

There were marked differences in the appearance between the embedded and free particles. As seen in the averaged profile of the embedded core complex shown in Fig. 3a, the cross-section of the wall was clearly asymmetrically broadened toward the outer side, Fig. 3b. In contrast, as seen in Fig. 3c, the free particles were much more strongly stained along the perimeter and their outer dimension appeared smaller (Fig. 3d). The appearance of the free particles matched very well the isolated core complexes from another FAP, *Roseiflexus castenholzii* (Collins et al. 2010), an important observation given the absence of detergent in our particle.

A peculiar feature of our samples was the appearance of the center of the embedded core complex particles. While some particles appeared to contain a weakly stained structure in the center, naturally interpreted as the RC, many gave a completely hollow appearance (Fig. 1), so that the resulting averaged particle classes appeared to be devoid of any structure in the center (Fig. 3a). Interestingly, the free complexes featured a weakly stained center region similar to the isolated complexes reported by Collins et al. (2010).

We found it unlikely that our method of sample preparation should cause loss of the RC from within the B808-B866 ring. However, there was the possibility of the presence of RC-free antenna complexes for example as an intermediate stage of the core complex assembly, or considering the similarity between the spectroscopic properties of the B808-866 complex and LH2, a RC-free antenna providing enhanced light-harvesting capacity.

Consequently, the question of the antenna to RC ratio in our samples and the possibility of the presence of B808-866 antenna rings lacking the RC were put to test using the light-induced oxidation of primary donor (P). We used rectangular light pulses produced by 850 nm LED. The duration of the actinic pulses was set to 1 s, and a series of experiments with various actinic intensities was done to determine the saturation intensity. A new sample was then used for the oxidation measurement. Full oxidation was reached within less than 200 ms, and the signal remained constant during the rest of the actinic pulse. The shape of the difference spectra corresponded to  $P^+$  oxidation published earlier (Pierson and Thornber 1983). In the dark, the  $P^+$  signal decayed with biexponential kinetics with the rate constant of the fast phase  $\sim 16$  s $^{-1}$  in a very good agreement with published value of rate constant of  $P^+Q_A^-$  recombination (Venturoli et al. 1991).

Assuming fixed RC to core antenna ratio, the amplitude of  $P$  spectrum bleaching at full  $P$  oxidation is linearly proportional to total absorbance. Then, using the assumption that

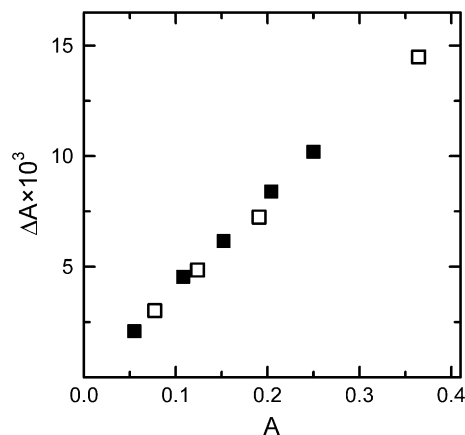


**Fig. 4** Plot of absorbance change due to the primary donor oxidation as a function of absorbance in *Cfx. aurantiacus* (measured at 866 nm, filled symbols) and *Rsp. rubrum* (measured at 875 nm, empty symbols) membranes diluted to different concentrations. The results show that the antenna: RC stoichiometry is likely very similar in the two species

the excitation coefficients for the antenna and the primary donor BChl  $a$  are approximately equal:

$$-\Delta A \approx \frac{2}{2N + 2} \times A \times k,$$

where  $k$  depends on the extinction coefficient of reduced and oxidized primary donor,  $k = (\varepsilon_P - \varepsilon_{P^+})/\varepsilon_P$ , and  $2N$  is the number (per RC) of antenna chlorophylls absorbing at given wavelength, e.g., at around 866 nm (monomeric B808 BChl  $a$ 's are not considered since they do not contribute to the absorption change around 866 nm); the dimeric nature of the primary donor is taken into account. Also, note that  $\Delta A < 0$ .

Based on the above, we obtained the information on the composition of *Cfx. aurantiacus* membrane in a straightforward manner, by comparing it to the cytoplasmic membrane of the purple bacterium *Rhodospirillum (Rsp.) rubrum*. This species is known to possess a 16-meric LH1 antenna complex (e.g., Jamieson et al. 2002). Moreover, occurrence of RC-less LH1 complexes in this species was reported to be infrequent (Fotiadis et al. 2004). In addition to that, due to the absence of the monomeric BChl  $a$  in the LH1 complex, the RC:LH1 stoichiometry can be assessed using the ratio of absorbance measured at 882 and 800 nm, as the latter peak is due solely to the accessory BChl  $a$  in the RC. This value in our samples was in agreement with earlier reports on the *Rsp. rubrum* core complex (Jamieson et al. 2002). As seen in Fig. 4, a very close correspondence between the results from *Cfx. aurantiacus* and *Rsp. rubrum* was found. This is consistent with 16-meric antenna complex in the former species. Moreover, the presence of a large number of antenna rings devoid of the RC in *Cfx. aurantiacus* could likely be excluded based on this

comparison. Hence, the intense staining of the centers of the core complexes embedded in the membrane that gave the appearance of a lack of RC was interpreted as an artifact of the staining procedure.

## Conclusions

The spatial arrangement of core complexes (B808-866-RC) in the native membranes of chlorosome-containing filamentous anoxygenic phototroph *Cfx. aurantiacus* was elucidated using electron microscopy of negatively stained samples. Typical nearest-neighbor center-to-center distance of ~18 nm was found, implying less protein crowding compared to membranes of purple bacteria. Moreover, it can be concluded that the association with chlorosome does not impose strict geometrical order upon the arrangement of core complexes. Using the spatial statistics derived from the images and chlorosome dimensions, mean RC:chlorosome ratio of 11 was estimated. Effect of irradiance upon the spatial distribution of core complexes was also demonstrated, resulting in changes of distribution of the distance to nearest-neighbor statistics. In addition, single-particle analysis of core complexes in the native membrane showed that the diameter of the core complex was about 50 % of the earlier estimate (Xin et al. 2005), while being in agreement with the more recent results from related species, *Rfx. castenholzii* (Collins et al. 2010).

**Acknowledgments** This research was supported by Czech Science Foundation P501/12/G055 (D.B., R.L., F.V.) and P205/11/1164 (Z.G.) and institutional support RVO:60077344. We thank Jeremy King, Aaron Collins, Jakub Pšenčík and the anonymous reviewers for helpful suggestions. Skilled technical assistance of František Matoušek is also gratefully acknowledged.

## References

- Adams PG, Cadby AJ, Robinson B, Tsukatani Y, Tank M, Wen J, Blankenship RE, Bryant DA, Hunter CN (2013) Comparison of the physical characteristics of chlorosomes from three different phyla of green phototrophic bacteria. *Biochim Biophys Acta* 1827:1235–1244
- Agarwal R, Rizvi AH, Prall BS, Olsen JD, Hunter CN, Fleming GR (2002) Nature of disorder and inter-complex energy transfer in LH2 at room temperature: a three pulse photon echo peak shift study. *J Phys Chem A* 106:7573–7578
- Bina D, Litvin R, Vacha F, Siffel P (2006) New multichannel kinetic spectrophotometer-fluorimeter with pulsed measuring beam for photosynthesis research. *Photosynth Res* 88:351–356
- Bina D, Litvin R, Vacha F (2010) Absorbance changes accompanying the fast fluorescence induction in the purple bacterium *Rhodobacter sphaeroides*. *Photosynth Res* 105:115–121
- Blankenship RE, Feick R, Bruce BD, Kirmaier C, Holten D, Fuller RC (1983) Primary photochemistry in the facultative green photosynthetic bacterium *Chloroflexus aurantiacus*. *J Cell Biochem* 22:1097–4644
- Cartron ML, Olsen JD, Sener M, Jackson PJ, Brindley AA, Qian P, Dickman MJ, Leggett GJ, Schulten K, Hunter CN (2014) Integration of energy and electron transfer processes in the photosynthetic membrane of *Rhodobacter sphaeroides*. *Biochim Biophys Acta*. <http://dx.doi.org/10.1016/j.bbabi.2014.02.003>
- Causgrove TP, Brune DC, Wang J, Wittmershaus BP, Blankenship RE (1990) Energy transfer kinetics in whole cells and isolated chlorosomes of green photosynthetic bacteria. *Photosynth Res* 26:39–48
- Collins AM, Qian P, Tang Q, Bocian DF, Hunter CN, Blankenship RE (2010) Light-harvesting antenna system from the phototrophic bacterium *Roseiflexus castenholzii*. *Biochemistry* 49:7524–7531
- Efron B (1979) Bootstrap methods: another look at the jackknife. *Ann Stat* 7:1–26
- Feick RG, Fitzpatrick M, Fuller RC (1982) Isolation and characterization of cytoplasmic membranes and chlorosomes from the green bacterium *Chloroflexus aurantiacus*. *J Bacteriol* 150:905–915
- Fetisova Z, Freiberg A, Novoderezhkin V, Taisova A, Timpmann K (1996) Antenna size dependent exciton dynamics in the chlorosomal antenna of the green bacterium *Chloroflexus aurantiacus*. *FEBS Lett* 383:233–236
- Fotiadis D, Qian P, Philippsen A, Bullough PA, Engel A, Hunter CN (2004) Structural analysis of the reaction center light-harvesting complex I photosynthetic core complex of *Rhodospirillum rubrum* using atomic force microscopy. *J Biol Chem* 279:2063–2068
- Frank J, Radermacher M, Penczek P, Zhu J, Li YH, Ladjadj M, Leith A (1996) SPIDER and WEB: processing and visualization of images in 3D electron microscopy and related fields. *J Struct Biol* 116:190–199
- Golecki JR, Oelze J (1987) Quantitative relationship between bacteriochlorophyll content, cytoplasmic membrane structure and chlorosome size in *Chloroflexus aurantiacus*. *Arch Microbiol* 148:236–241
- Hohmann-Marriott MF, Blankenship RE (2007) Hypothesis on chlorosome biogenesis in green photosynthetic bacteria. *FEBS Lett* 581:800–803
- Hsin J, Chandler DE, Gumbart J, Harrison CB, Sener M, Strumpfer J, Schulten K (2010) Self-assembly of photosynthetic membranes. *Chem Phys Chem* 11:1154–1159
- Huh J, Saikin SK, Brookes JC, Valteau S, Fujita T, Aspuru-Guzik A (2014) Atomistic study of energy funneling in the light-harvesting complex of green sulfur bacteria. *J Am Chem Soc* 136:2048–2057
- Jamieson SJ, Wang PY, Qian P, Kirkland JY, Conroy MJ, Hunter CN, Bullough PA (2002) Projection structure of the photosynthetic reaction centre-antenna complex of *Rhodospirillum rubrum* at 8.5 Å resolution. *EMBO J* 21:3927–3935
- Kirchhoff H (2008) Molecular crowding and order in photosynthetic membranes. *Trends Plant Sci* 13:201–207
- Majumder ELW, King JD, Blankenship RE (2013) Alternative complex III from phototrophic bacteria and its electron acceptor auracyanin. *Biochim Biophys Acta* 1827:1383–1391
- Miller KR (1979) Structure of a bacterial photosynthetic membrane. *Proc Natl Acad Sci USA* 76:6415–6419
- Montano GA, Wu H-M, Lin S, Brune DC, Blankenship RE (2003) Isolation and characterization of the B798 light-harvesting baseplate from the chlorosomes of *Chloroflexus aurantiacus*. *Biochemistry* 42:10246–10251
- Muller MG, Griebenow K, Holzwarth AR (1993) Picosecond energy transfer and trapping kinetics in living cells of the green bacterium *Chloroflexus aurantiacus*. *Biochim Biophys Acta* 1144:161–169
- Olsen JD, Tucker JD, Timney JA, Qian P, Vassilev C, Hunter CN (2008) The organization of LH2 complexes in membranes from *Rhodobacter sphaeroides*. *J Biol Chem* 283:30772–30779



- Ovchinnikov YA, Abdulaev NG, Zolotarev AS, Shmukler BE, Zargarov AA, Kutuzov MA, Telezhinskaya IN, Levina NB (1988a) Photosynthetic reaction centre of *Chloroflexus aurantiacus*. I Primary structure of L-subunit. FEBS Lett 231:237–242
- Ovchinnikov YA, Abdulaev NG, Shmuckler BE, Zargarov AA, Kutuzov MA, Telezhinskaya IN, Levina NB, Zolotarev AS (1988b) Photosynthetic reaction centre of *Chloroflexus aurantiacus*. II Primary structure of M-subunit. FEBS Lett 232:364–368
- Pedersen MO, Linnanto J, Frigaard NU, Nielsen NC, Miller M (2010) A model of the protein-pigment baseplate complex in chlorosomes of photosynthetic green bacteria. Photosynth Res 104:233–243
- Pierson BK, Thornber JP (1983) Isolation and spectral characterization of photochemical reaction centers from the thermophilic green bacterium *Chloroflexus aurantiacus* J-10-fl. Proc Natl Acad Sci USA 80:80–84
- Psencik J, Collins AM, Liljeroos L, Torkkeli M, Laurinmäki P, Ansink HM, Ikonen TP, Serimaa RE, Blankenship RE, Tuma R, Butcher SJ (2009) Structure of chlorosomes from the green filamentous bacterium *Chloroflexus aurantiacus*. J Bacteriol 191:6701–6708
- Roszak AW, Howard TD, Southall J, Gardiner AT, Law CJ, Isaacs NW, Cogdell RJ (2003) Crystal structure of the RC-LH1 core complex from *Rhodospseudomonas palustris*. Science 302:1969–1972
- Scheuring S, Seguin J, Marco S, Levy D, Robert B, Rigaud JL (2003) Nanodissection and high-resolution imaging of the *Rhodospseudomonas viridis* photosynthetic core complex in native membranes by AFM. Proc Natl Acad Sci USA 100:1690–1693
- Scheuring S, Levy D, Rigaud JL (2005) Watching the components of photosynthetic bacterial membranes and their in situ organisation by atomic force microscopy. Biochim Biophys Acta 1712:109–127
- Tang KH, Urban VS, Wen J, Xin Y, Blankenship RE (2010) SANS investigation of the photosynthetic machinery of *Chloroflexus aurantiacus*. Biophys J 99:2398–2407
- Venturoli G, Trotta M, Feick R, Melandri BA, Zannoni D (1991) Temperature dependence of charge recombination from the  $P^+QA^-$  and  $P^+QB^-$  states in photosynthetic reaction centers isolated from the thermophilic bacterium *Chloroflexus aurantiacus*. Eur J Biochem 202:625–634
- Wittmershaus BP, Brune DC, Blankenship RE (1988) Energy transfer in *Chloroflexus aurantiacus*: Effects of temperature and anaerobic conditions. In: Scheer H, Schneider S (eds) Photosynthetic light-harvesting systems. Walter de Gruyter, Berlin, pp 543–554
- Xin Y, Lin S, Montano G, Blankenship RE (2005) Purification and characterization of the B808-866 light-harvesting complex from green filamentous bacterium *Chloroflexus aurantiacus*. Photosynth Res 86:155–163